Large-Scale Rate-Splitting Multiple Access in Uplink UAV Networks: Effective Secrecy Throughput Maximization Under Limited Feedback Channel

Hamed Bastami, Hamid Behroozi, *Member, IEEE,* Majid Moradikia, Ahmed Abdelhadi, Derrick Wing Kwan Ng and, *Fellow, IEEE*, and Lajos Hanzo, *Life Fellow, IEEE*

***Abstract*—Unmanned aerial vehicles (UAVs) are capable of improving the performance of next generation wireless systems. However, their communication performance is prone to both channel estimation errors and potential eavesdropping. Hence, we investigate the effective network secrecy throughput (ENST) of the uplink UAV network, in which rate-splitting multiple access (RSMA) is employed by each legitimate user for secure transmission under the scenario of massive access. To maximize the ENST, the transmission rate versus power allocation relationship is formulated as a max-min optimization problem, relying on realistic imperfect channel state information (CSI) of both the legitimate users and passive eavesdroppers ($Eves$). In the model considered, each user transmits a superposition of two messages to a UAV base-stations (UAV-BS), each having different transmit power and the UAV-BS adopts a successive interference cancellation (SIC) technique to decode the received messages. Given the non-convexity of the problem, it is decoupled into a pair of sub-problems. In particular, we derive a closed form expression for the optimal rate-splitting fraction of each user. Then, given the optimal rate-splitting fraction of each user, the ϵ-constrainted transmit power of each user is calculated by harnessing sequential parametric convex approximation (SPCA) programming. Our simulation results confirm that the scheme conceived significantly improves the ENST compared to both the existing orthogonal and non-orthogonal benchmarks.**

***Index Terms*—Rate-splitting, PLS, effective network secrecy throughput, imperfect CSIT, worst-case optimization.**

I. Introduction

In order to support the emerging Beyond fifth-generation (B5G) system concept, unmanned aerial vehicles (UAV) may be harnessed as air-borne base-station (BS), particularly in the areas of high tele-traffic density [1]-[6]. However, owing to their line-of-sight (LoS) propagation UAV-BSs usually suffer from strong co-channel interference. Although this problem can be potentially mitigated by the sophisticated trajectory design of UAVs [1], [2], the degrees of freedom attained is typically inadequate to support the ever-growing terrestrial user population. In this context, multiple access (MA) techniques play a crucial role in fulfilling the high data rate, low latency, and massive connectivity requirements, as the three most important Key Performance Indicators (KPI)s for B5G [3]-[14].

Rate-splitting multiple access (RSMA) has attracted a great deal of interest, as a key-enabling radio access technology capable of satisfying the massive connectivity requirements of B5G [3], [5], [6], [9]-[14]. Briefly, RSMA is a generalization of non-orthogonal multiple access (NOMA) and space-division multiple access (SDMA) [9], that outperforms both schemes in terms of its robustness and spectral efficiency. In a rate-splitting (RS) scheme, the transmitted signals are split into two parts at the transmitter (Tx) [29], namely into a common message and a private message. Subsequently, by performing successive interference cancellation (SIC) at the receiver (Rx), the capacity region of the MA channel (MAC) can be approached without the need for time sharing among users [13], [29], [30][1]. Inspired by this promising MA framework, most of the RSMA-based literature considered the downlink (DL) [3], [5], [6], [9], [10] even though the DL actually represents a broadcast scenario and multiple access is only possible in the uplink (UL). In [11] a RS scheme was designed for guaranteeing max-min fairness in UL-NOMA. As a further advance, a cooperative rate-splitting (CRS) UL scheme was proposed in [12], where each user broadcasts his/her signal during the first phase and receives the transmitted signal of the other user, while during the second phase, each user relays the other user's message. Then, Yang *et al*. [14], proposed UL-RSMA for maximizing the users' sum-rate by optimally sharing the total transmit powers of both user-messages, while exhaustively searching for the optimal decoding order at the SIC receiver. In [15], the outage performance of the RSMA UL supporting randomly deployed users is investigated, taking both user scheduling schemes and power allocation strategies into consideration. Also, an intelligent reflecting surface (IRS) aided UL RSMA system is investigated in [16] for dead-zone users, where the direct link between the users and the BS is unavailable and the UL transmission is considering only through IRS. In [16]the problem of sum-rate maximization is formulated for jointly design the optimal power allocation at each UL user and the passive beamforming at the IRS under the optimal decoding order of sub-messages. However, these contributions stipulate the idealized simplifying assumption of having perfect channel state information (CSI) for resource allocation design, which is not realistic in practice. More particularly, in massive access scenarios in which a large number of CSIs have to be reported to the BS using limited feedback having CSI imperfections is unavoidable, resulting in link outage [8], [17]. More importantly, none of the above-

L. Hanzo would like to acknowledge the financial support of the Engineering and Physical Sciences Research Council projects EP/W016605/1 and EP/X01228X/1 as well as of the European Research Council's Advanced Fellow Grant QuantCom (Grant No. 789028)

[1]Note that there are three methods that can achieve the capacity region, namely joint encoding/decoding, time sharing, and rate splitting. Joint encoding/decoding is not practical due to the high complexity of code construction and joint decoding at the receiver. The second method namely, time sharing, imposes extra communication overheads and stringent synchronization requirements due to the coordination of the transmissions of all the users. Finally, due to the lack of time sharing, RSMA allows one to achieve the capacity region at comparatively low signaling overhead [13], [29], [30].

mentioned RSMA UL scenarios of [11]-[14] have addressed the associated security concerns. In particular, the concurrent UL transmissions of a massive number of messages over the same bandwidth increases the risk of security breaches. To protect the confidentiality of the transmitted signals, physical layer security (PLS) techniques can be exploited for increasing the channel capacity difference between the legitimate and eavesdropping links. Unfortunately, MA systems are particularly susceptible to passive attacks, since the eavesdroppers ($Eves$) have more target users, they can glean information from [5], [8], [10]. In this context, jamming aims for confusing the potential $Eves$ by deliberately injecting specifically designed artificial noise (AN) with the aid of beamforming [18], [19]. As a further development, the authors of [20], [21] proposed a secure NOMA approach. In fact, after detecting the superimposed streams Eve becomes capable of wiretapping the rest of the embedded information, which is becoming less interference-infested. By contrast, using an RSMA scheme, the common message plays the dual roles of the desired message as well as that of the AN without the need for assigning a portion of the limited transmit power to the AN [5], [6], [10]. However, the secure RSMA designs of [5], [6], [10] considered the DL scenario, hence their results are not applicable to the UL due to the different nature of the problems. To the best of our knowledge, at the time of writing, no attention has been devoted to the integration of UL-RS with UAV-BS. Furthermore, the robust and secure design of RSMA-aided UAV networks relying on realistic imperfect CSI has not been investigated so far.

Given the knowledge gaps mentioned above, we consider a network in which the legitimate users aim for communicating with a UAV-BS in the presence of multiple passive Eve. In this UL scenario, each user employs RS, where the corresponding message of each user is split into two parts. Then, each user transmits a superposition of two messages having different power levels. To realize massive connectivity, we assume furthermore that at the network initialization a clustering process is accomplished by which the users are divided into different non-overlapping groups. Furthermore, due to the limited CSI feedback accuracy, a link outage may occur. Hence we introduce a maximum tolerable connection outage probability (COP) constraint for quantifying its impact on the system performance. It is worth mentioning that in contrast to the RSMA downlink in [5], [10], where the authors considered the secure design of the common streams, here we exploit a different strategy, where the transmission rate and the power allocated to each part of the bipartite messages is optimized in terms of *Effective Network Secrecy Throughput* (ENST) maximization. ENST is a secrecy performance metric quantifying the average secure throughput. More explicitly, when the reception reliability is considered to be similarly important to the security, then this parameter is considered. Mathematically, ENST is formulated as the product of the target secrecy rate and the probability of successful reception. Against this background, our contributions are summarized as follows:

- In addition to the COP constraint, which captures the impact of link outages, the secrecy outage probability (SOP) is tightly controlled to be under the tolerable level under unknown CSI of the Eve. We then maximize the ENST, subject to both COP and SOP constraints, as well as to the limited power budget. In particular, we design the RS power allocation at the users as well as the SIC-ordering corresponding to each cluster, so that the ENST is maximized.
- To deal with the resultant non-convex problem, we first derive a closed-form expression for characterizing the COP and a tight approximation of the SOP constraints. Then, we harness the two-tier block coordinate decent technique, where the optimization variables are estimated successively in an iterative manner. The first loop of this twin-tier approach maximizes the transmission rates, leading to a closed-form optimal solution relying on the Lambert W-function. By contrast, the second loop encounters some non-convexities, which are tackled by the powerful sequential parametric convex approximation (SPCA) method. The convex approximation of the non-convex factors are found with the aid of the first-order Taylor expansion.
- Our simulation results demonstrate that the proposed framework outperforms the existing non-orthogonal benchmarks in terms of the ENST criterion.

Our contributions are boldly and explicitly contrasted to the state-of-the-art at a glance in Table 1. The rest of this paper is organized as follows. The system model and channel definitions are provided in Section II. Section III describes the signal representation and formulates our ENST maximization problem. The proposed SPCA-based solution, the two-tier block coordinate decent procedures and our complexity analysis are provided in Section IV. In Section V, our simulation results are presented and the paper is concluded in Section VI. Finally, the Appendices and Proofs of the claims are provided in Section VII.

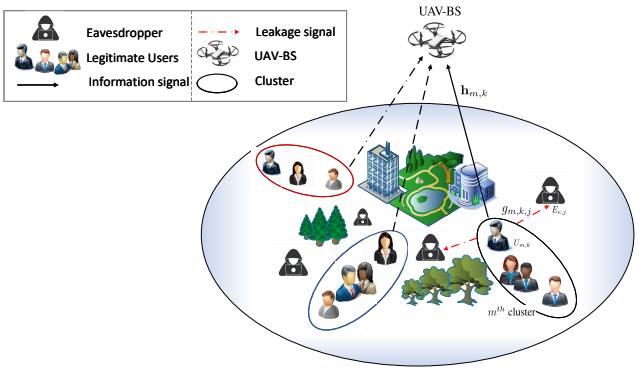

Fig. 1. The considered system model adopting RSMA.

Notation: Vectors and matrices are denoted by lower-case and upper-case boldface symbols, respectively; $(.)^{\mathrm{T}}$, $(.)^{*}$, $(.)^{\mathrm{H}}$, and $(.)^{-1}$ denote the transpose, conjugate, conjugate transpose, and inverse of a matrix respectively; $\Re e(.)$ denotes the real part of a complex variable, and $\Im m(.)$ the imaginary part of a complex variable; We use $\mathbb{E}\{\cdot\}$ and $\triangleq$ to denote the

TABLE I
BOLDLY AND EXPLICITLY CONTRASTING OUR CONTRIBUTIONS TO THE EXISTING LITERATURE.

References⇒ / Keywords⇓	**Our Approach**	[1]	[2]	[3]	[4]	[5]	[6]	[7]	[8]	[9]	[10]	[11]	[12]	[14]	[17]	[18]	[19]	[20]	[21]
UAV-BS	✓	✓	✓	✓	✓	✓	✓				✓								
UAV Trajectory Design		✓	✓																
IUI Management		✓	✓			✓	✓	✓											
IUI Cancellation	✓													✓					
RSMA	✓			✓		✓	✓			✓	✓	✓	✓	✓					
NOMA									✓									✓	✓
SDMA								✓											
Limited Feedback Error	✓							✓	✓						✓				
Imperfect CSI	✓					✓	✓		✓		✓				✓			✓	
Known Eve with Imperfect E-CSIT						✓	✓				✓							✓	
Max-Min Fairness						✓	✓				✓	✓							
Sum-Rate Maximization									✓					✓					
Unknown Eve	✓															✓			
ICI Cancellation	✓																		
ENST Maximization	✓																		
COP Constraint	✓																		
SOP Constraint	✓																		

expectation operation and a definition, respectively. A complex Gaussian random variable with mean μ and variance σ^2 reads as $\mathcal{CN}\left(\mu,\sigma^2\right)$, and $\text{Exp}\left(\lambda\right)$, $\text{Beta}\left(\alpha,\beta\right)$, and $\text{Gamma}\left(\gamma,\zeta\right)$ respectively denote the exponential distribution with mean λ, beta-distribution with parameters α and β, and gamma-distribution with shape γ and rate ζ. The principal branch of the Lambert W-function is defined by $W_0\left(x\right)e^{W_0(x)} = x$ for $x \geq -\frac{1}{e}$ with $W_0\left(x\right) \geq -1$ [22]; $\mathbf{I}_N$ denotes the $N \times N$ identity matrix; The notations $\left[x\right]^+$ and $\mathbb{P}\left(.\right)$ stand for $\max\{x, 0\}$ and probability, respectively. The entry in the i-th row of a vector $\mathbf{h}$ is represented by $\mathbf{h}\left[i\right]$. Furthermore, $\mathbf{u}^{max}\left\{\mathbf{A}\right\}$ and $\mathbf{v}^{max}\left\{\mathbf{A}\right\}$ denote the columns of $\mathbf{U_A}$ and $\mathbf{V_A}$ corresponding to the dominant singular value $\lambda^{max}\left\{\mathbf{A}\right\}$ of matrix $\mathbf{A}$, respectively, i.e., the matrix $\mathbf{A}$ has a Singular Value Decomposition (SVD) given by $\mathbf{A} \triangleq \mathbf{U_A}\mathbf{\Lambda_A}\mathbf{V_A}$. Finally, $\angle\left(\mathbf{u},\mathbf{v}\right)$ represents the angle between vectors $\mathbf{v}$ and $\mathbf{u}$.

II. SYSTEM MODEL

We consider the secure single-input multi-output (SIMO) uplink system, shown in Fig. 1. There are M clusters in the network considered, whose m^{th} cluster includes K_m number of single-antenna legitimate users gathered in the set $\boldsymbol{U}_m \triangleq \{U_{m,k}\}$, $\forall k \in \mathcal{K}_m \triangleq \{1,\ldots,K_m\}$, who aim for transmitting to an N_t-antenna UAV-BS. We consider a massive access setting, where $\sum_{m=1}^{M} K_m \gg M$. Meanwhile, J number of non-cooperative passive N_e-antenna eavesdroppers ($Eves$) gathered in the set $\boldsymbol{E} \triangleq \{E_{e,j}\}, \forall j \in \mathcal{J} \triangleq \{1,\ldots,J\}$, manage in covert wiretapping[2]. Next, the channel models and the clustering procedure operating under CSI error are described.

[2]In this paper we have focused on non-colluding Eve's who try to maximize their own SINR individually. The problem of colluding $Eves$ has been left for future work.

A. Channel Definitions

In our scenario, the $U_{m,k} \longrightarrow E_{e,j}$ channels are represented by $\mathbf{q}_{m,j,k},\ \forall m,\ k,\ j$, while the legitimate channels spanning from the terrestrial user to the UAV-BS, i.e., $U_{m,k} \longrightarrow UAV$, are denoted by $\mathbf{h}_{m,k}\ \forall m,k$. The ground-to-air (G2A) channels are modeled by $\mathbf{h}_{m,k} = \sqrt{PL\left(d_{m,k}\right)}\,\mathbf{f}_{m,k}$, where $PL\left(d_{m,k}\right) \triangleq {d_{m,k}}^{-\alpha_{m,k}}$ represents the large-scale fading, while $d_{m,k}$ and $\mathbf{f}_{m,k} \sim \mathcal{CN}\left(0,\mathbf{I}_{N_t}\right)$ therein, respectively, denote the G2A distance and the corresponding small-scale fading. The path-loss exponent $\alpha_{m,k}$ obeys the probabilistic model [23], which is appropriate for low-altitude UAVs comprised of both the LoS and non-LoS channels.

B. Clustering Under CSI Error

Given the slowly time-varying nature of the $PL\left(d_{m,k}\right)$, we assume that both the UAV as well as the users can estimate it perfectly. However, due to the limited hardware complexity of the UAV, we assume that the UAV only captures the angle-of-arrival (AoA) information of the user-UAV channel, and even this AoA information is imperfect. To elaborate a little further, first the UAV broadcasts a sequence of training symbols towards the ground users, who aim for acquiring the knowledge of their own DL channels. In general, given a sufficiently high transmit power, as well as a long training sequence, legitimate users are capable of perfectly estimating their own channels. More explicitly, all the users within the m^{th} cluster have the same AoA and thus we can construct a codebook $\mathcal{V}$, comprised of M unit-norm vectors $\{\mathbf{v}_m\}_{m=1}^{M} \in \mathbb{C}^{N_t \times 1}$. At the network's initialization, this codebook is randomly generated and made known off-line to both the UAV and the users for example via the codebook distribution regime

1	Formulating the ENST maximization with COP and SOP constraints in Eq. (11), aimed at optimizing $S \triangleq \{r_{m,k,n} \geq 0,\ D_{j,k,n} \geq 0, P_{m,k,n} \geq 0, \Phi_{\mathrm{m}}\ \}$.
2	Reformulating the problem in (15), based on the closed-form COP constraint (12) and tight SOP constraint (14).
3	First tier of block-coordinate decent, including the estimation of $\{r_{m,k,1}, r_{m,k,2}\}_{\mathrm{k=1}}^{K_M}$, while keeping the other parameters fixed through solving the problem (16). The closed form solution then was acquired in (18).
4	Second tier of block-coordinate decent, including the estimation of $\{r_{m,k,n} \geq 0,\ D_{j,k,n} \geq 0\ \}_{\mathrm{k=1}}^{K_M}$, while keeping $\{r_{m,k,1}, r_{m,k,2}\}_{\mathrm{k=1}}^{K_M}$ fixed. Due to non-convexity, we have resorted to SPCA, resulting in the ϵ-constraint solution through solving problem (30), encompassing the affine-approximated constraints (30-C1) -(30-C3).
5	Overall algorithm iterates between the outer (first tier) and inner tiers (first tier). By substituting the optimal point $\{r^*_{m,k,n} \geq 0,\ D^*_{j,k,n} \geq 0\ \}_{\mathrm{k=1}}^{K_M}$ calculated from the inner loop, the $(q+1)$-st iteration of the outer loop updates ϵ-constraint solution $\{r^*_{m,k,1}, r^*_{m,k,2}\}_{\mathrm{k=1}}^{K_M}$ according to (31).

Fig. 2. The algorithmic procedure of the proposed method

of [25]. To convey the corresponding AoA to the UAV, each $U_{m,k}$ quantizes its channel direction, i.e., $\widetilde{\mathbf{f}}_{m,k} \triangleq \frac{\mathbf{f}_{m,k}}{\|\mathbf{f}_{m,k}\|}$, to the closest vector in terms of the chordal distance metric of [26], [27]:[3]

$$\hat{\mathbf{f}}_{m,k} \triangleq \arg\max_{\mathbf{v}_m \in \mathcal{V}} \left|\widetilde{\mathbf{f}}_{m,k}^H \mathbf{v}_m\right|^2 = \arg\max_{\mathbf{v}_m \in \mathcal{V}} \cos^2\left[\angle\left(\widetilde{\mathbf{f}}_{m,k}, \mathbf{v}_m\right)\right]. \tag{1}$$

Accordingly, the users having the maximum chordal distance between their so-obtained channel direction $\widetilde{\mathbf{f}}_{m,k}$ and $\mathbf{v}_m$ are allocated to the m^{th} cluster and the number of users within each cluster, i.e., K_m, is also updated after the grouping. Now, each user sends the corresponding codebook index back to the UAV using $B \triangleq \lceil \log_2 M \rceil$ bits through an error-free and delay-free feedback channel. However, because of the limited feedback per channel coherence block as well as the instability of the UAV platform, the CSI of the main channel obtained at the UAV is imperfect. Thus, a quantization error in the form of

$$\widetilde{\mathbf{f}}_{m,k} = \cos(\phi_{m,k})\,\hat{\mathbf{f}}_{m,k} + \sin(\phi_{m,k})\,\mathbf{e}_{m,k}, \tag{2}$$

appears in the AoA estimates of users, where $\mathbf{e}_{m,k} \in \mathbb{C}^{N_t \times 1}$ is the unit-norm quantization error vector isotropically distributed in the null-space of $\widetilde{\mathbf{f}}_{m,k}$, while $\phi_{m,k} \triangleq \angle\left(\widetilde{\mathbf{f}}_{m,k}, \mathbf{v}_m\right)$ of (2) represents the angle between $\widetilde{\mathbf{f}}_{m,k}$ and $\mathbf{v}_m$, and $\sin^2(\phi_{m,k})$ being a random variable, whose variance is determined by B [28]. To visualize the proposed approach, the whole procedure is shown in Fig. 2, while further details will be presented in the sequel.

[3]The optimal vector quantization strategy in multi-user uplink channels, even in single-cell systems, is not known in general and it is beyond the scope of our work.

III. Signal Representation and Problem Formulation

In the RSMA uplink, each $U_{m,k}$ within the m^{th} cluster transmits a superposition code of two normalized sub-messages $s_{m,k,n}|_{n=1}^2$, i.e., $\mathbb{E}\left\{|s_{m,k,n}|^2\right\} = 1$, given by [30]:

$$s_{m,k} = \sum_{n=1}^{2} \sqrt{p_{m,k,n}}\, s_{m,k,n},\ \forall k \in \mathcal{K}_m, \tag{3}$$

where $p_{m,k,n}$, $\forall n \in \{1,2\}$ corresponds to the transmit power of $s_{m,k,n}\, \forall n \in \{1,2\}$. During the uplink signal reception, the UAV relies on beamforming for discriminating the signals received by suppressing the IUI. Therefore, the signal received at the UAV, i.e., y_{UAV}, is passed through M different angularly selective filters $\{\mathbf{w}_m\}_{m=1}^M \in \mathbb{C}^{N_t \times 1}$, distributed in M branches. Accordingly, the m^{th} signal (i.e., the m^{th} branch) received by the UAV and the received signal at $Eves$, respectively denoted by $y_{UAV,m}$ and $y_{e,j}$, are formulated as follows:

$$y_{\mathrm{UAV},m} = \mathbf{w}_m^H \left(\sum_{i=1}^{M}\left(\sum_{k=1}^{K_i} \mathbf{h}_{i,k} s_{i,k}\right) + \mathbf{z}\right), \tag{4}$$

$$y_{e,j} = \mathbf{w}_{m,j}^H \left(\mathbf{Q}_{m,j}\mathbf{s}_m + \mathbf{z}_{m,j}\right), \forall j \in \mathcal{J}, \tag{5}$$

where $\mathbf{Q}_{m,j} \triangleq [\mathbf{q}_{m,j,1}, \mathbf{q}_{m,j,2}, ..., \mathbf{q}_{m,j,K}]$, $\mathbf{s}_m \triangleq [s_{m,1}, s_{m,2}, ..., s_{m,K}]^T$, $z_m \triangleq \mathbf{w}_m^H \mathbf{z}_m \sim \mathcal{CN}(0, \sigma_m^2)$

and $\mathbf{z}_{m,j} \sim \mathcal{CN}\left(0, \sigma_e^2 \mathbf{I}_{N_e}\right)$ represent the additive white Gaussian noise (AWGN) due to the m^{th} cluster at the UAV and at the j^{th} Eve, respectively. $\mathbf{w}_{m,j} \triangleq \mathbf{u}^{max}\left\{\tilde{\mathbf{Q}}_{m,j}\right\}$ represents the MRC beamformer employed by Eve where $\tilde{\mathbf{Q}}_{m,j} \triangleq \mathbf{Q}_{m,j}\left(\mathbf{Q}_{m,j}\right)^H$. It is easy to show that $y_{e,j} = \sum_{k=1}^{K_m} g_{m,k,j} s_{m,k} + \xi_{e,j}$, $\forall j \in \mathcal{J}$, where $g_{m,k,j} \sim \mathcal{CN}\left(0, \sqrt{\lambda_j^{max}\left\{\tilde{\mathbf{Q}}_{m,j}\right\}}\right)$ [24], and $\xi_{e,j} \sim \mathcal{CN}\left(0, \sigma_e^2\right)$. In terms of the worst-case secrecy scenario, Eve is assumed to be able to perfectly estimate its corresponding CSI and no ICI is available to degrade the performance of Eve. To force the ICI terms to zero, we resort the zero-forcing (ZF) beamforming. More explicitly, upon relying on the codebook $\mathcal{V}$ discussed earlier in Section I.B, $\mathbf{w}_m$ is chosen so that we have $\mathbf{w}_m^H \mathbf{v}_l = 0$, $\forall l \neq m$, $l \in \{1, 2, ..., M\}$.

When considering the signal extracted from the m^{th} cluster, the UAV employs $2K_m$ number of SIC stages to suppress IUI as well as to decode all transmitted messages in the set $\mathcal{K}_{m,n} \triangleq \{s_{m,k,n}\}$ received from $y_{\text{UAV},m}$. The decoding order of the m^{th} cluster at the UAV is denoted by a permutation $\mathbf{\Phi}_m$, which belongs to set $\mathbf{\Pi}_m$ defined as the set of all possible decoding orders of all $2K_m$ messages arriving from K_m users, which includes $\frac{2K_m!}{2^{K_m}}$ elements. Let $\Phi_{m,k,n}$ represents the position of the message $s_{m,k,n}$ in $\mathbf{\Phi}_m$. Therefore, we can define $\Phi_{m,k,n} = \{(k',n') \neq (k,n) | (k',n') \succ (k,n)\}$, where the operator $(k',n') \succ (k,n)$ indicates that $s_{m,k,n}$ has a higher decoding order than $s_{m,k',n'}$ in $\mathbf{\Phi}_m$, i.e., the UAV is scheduled to decode $s_{m,k',n'}$ after decoding and cancelling out the effect of $s_{m,k,n}$.

Therefore, in the SIC scheme of the RSMA uplink, the UAV first decodes and subtracts the remodulated signals having higher decoding orders. i.e., $(k',n') \in \mathcal{K}_{m,n} \setminus \{(k,n) \bigcup \Phi_{m,k,n}\}$, then it decodes signal $s_{m,k,n}$, where the signal of the users in $\Phi_{m,k,n}$ is treated as noise. According to the SIC protocol, the signal of $s_{m,k,n}$ will be decoded prior to $s_{m,k',n'}$ if we have $|\Phi_{m,k,n}| > |\Phi_{m,k',n'}|$, where $|\mathcal{A}|$ is the cardinality of the set $\mathcal{A}$. Accordingly, the signal-to-interference-plus-noise ratio (SINR) at the UAV experienced upon detecting $s_{m,k,n}$, and denoted by $\rho_{m,k,n}$ is formulated as (6), where the IUI and ICI terms are obtained by substituting (3) into (6). Notably, after clustering in the presence of beamforming weight quantization errors the ICI cannot be completely removed by the beamformer having the weights of $\mathbf{w}_m$, thus a residual ICI term contaminates the corresponding received signal of the m^{th} cluster. In other words, the beamformer weights $\mathbf{w}_m$ fail to perfectly null out the ICI due to the limited feedback.

Furthermore, it is assumed that the $Eves$ have no information about $\mathbf{\Phi}_m$, hence they cannot perform SIC within a cluster [4]. Consequently, from the perspective of $E_{e,j}$, the received SINR of decoding $s_{m,k,n}$, while treating the other ones as noise, is formulated as:

$$\mu_{j,k,n} = \frac{p_{m,k,n} \text{PL}\left(d_{m,k,j}\right) |g_{m,k,j}|^2}{\sum_{(k',n') \neq (k,n)} p_{m,k',n'} \text{PL}\left(d_{m,k',j}\right) |g_{m,k',j}|^2 + \sigma_e^2}. \quad (7)$$

[4]As a more challenging secrecy scenario, for comparison, in our simulation we consider a scenario when $E_{e,j}$ can exploit the optimal SIC decoding order and receives no CSI.

Given the SINRs in (6) and (7), the corresponding achievable rates are respectively given by $C_{m,k,n} \triangleq \log_2\left(1 + \rho_{k,m,n}\right)$ and $C_{j,k,n} \triangleq \log_2\left(1 + \mu_{j,m,n}\right)$.

Remark 1. For ensuring reliable uplink communication, the transmission rate $r_{m,k,n}$ of each $U_{m,k}$ should not exceed $C_{m,k,n}$, i.e., $C_{m,k,n} \geq r_{m,k,n}$. However, as a consequence of ICI and fading, $r_{m,k,n}$ might violate this condition, hence leading to the link outages. However, the COP, defined as the probability that a system is unable to support the target transmission rate $C_{m,k,n}$, must be limited by the maximum tolerable COP $\epsilon_{cop} \in (0,1)$, as follows:

$$\text{COP}: \qquad P_{m,k,n}^{CO} \triangleq \mathbb{P}\left\{r_{m,k,n} > C_{m,k,n}\right\} \leq \epsilon_{cop}. \quad (8)$$

Remark 2. On the other hand, since the $U_{m,k}$ has no knowledge concerning the CSIs of passive $Eves$ [32], the values of $\mu_{j,m,n}$ are unknown. A beneficial secrecy policy in this situation is to adjust the redundancy rate of $U_{m,k}$ [32], denoted by $D_{j,k,n}$, so that the COP limit of (8) is satisfied[5]. In other words, $D_{j,k,n}$ must not exceed $C_{j,k,n}$. To do so, the SOP of $\epsilon_{sop} \in (0,1)$, satisfies: [6]

$$\text{SOP}: \qquad P_{j,k,n}^{SO} \triangleq \mathbb{P}\left\{D_{j,k,n} \leq C_{j,k,n}\right\} \leq \epsilon_{sop}. \quad (9)$$

Remark 3. Upon considering non-colluding $Eves$, the achievable secrecy rates of $U_{m,k}$ where transmitting $s_{k,m,n}$ is limited by the worst-case Eve scenario of $C_{m,k,n}^{sec} \triangleq \min_{1 \leq j \leq J}\left\{[r_{m,k,n} - D_{j,k,n}]^+\right\}$. On the other hand, while minimizing $P_{m,k,n}^{CO}$ would improve the reliability, maximizing $C_{m,k,n}^{sec}$ will enhance the security upon jointly considering both the reliability and security requirements of all $U_{m,k}|_{k=1}^{\mathcal{K}_m}$, we should rather maximize the ENST, defined as $C_{ENST} \triangleq \sum_{k=1}^{K_m} \sum_{n=1}^{2} \left(1 - P_{m,k,n}^{CO}\right) C_{m,k,n}^{sec}$.

Based on the discussion in Remarks 1-3, while considering the limited power budget imposed on each $U_{m,k}$, formulated as $\sum_{n=1}^{2} p_{m,k,n} \leq P_{m,k}$, the optimization problem of the proposed secure RSMA-based uplink is formulated as:

$$\max_{\mathcal{S}} \left(\min_{1 \leq j \leq J} \left\{ \sum_{k=1}^{K_m} \sum_{n=1}^{2} \left(1 - P_{m,k,n}^{CO}\right) [r_{m,k,n} - D_{j,k,n}]^+ \right\} \right) \quad (10)$$

s.t.

$$C_1: (8),\ C_2: (9),\ C_3: \sum_{n=1}^{2} p_{m,k,n} \leq P_{m,k},\ p_{m,k,n} \geq 0,$$

$\forall k, j$, where $\mathcal{S} \triangleq \{r_{m,k,n} \geq 0,\ D_{j,k,n} \geq 0,\ p_{m,k,n} \geq 0,\ \Phi_m\}$. Due to the non-convex objective function (OF), as well as

[5]A wiretap code can be designed by choosing two code rates, namely, the codeword rate, R_B, and the rate of transmitted confidential information (or equivalently, the target secrecy rate) R_s. The redundancy rate, $R_E \triangleq R_B - R_s$, is exploited to confuse Eve. In order to meeting the reliability constraint of wiretap channels, the rate of transmitted codewords has to be chosen as $R_B \leq C_B$, where C_B is the capacity of the main channel. In order to guarantee the secrecy constraint of wiretap channels, the redundancy rate has to be chosen as $R_E > C_E$, where C_E is the capacity of Eve's channel. If the values of both C_B and C_E are available at Alice, the maximum target secrecy rate is also achievable, which is referred to as the secrecy capacity of a wiretap channel and it is given by $C_S \triangleq C_B - C_E$ [29].

[6]It should be highlighted that, we considered the worst-case condition for ensuring both reliability and security of each part of split messages. This implies that if actual transmission rate of each split messages $s_{m,k,n}\ \forall n \in \{1,2\}$ corresponding to $U_{m,k}$ can satisfy its target transmission rate $C_{m,k,n}\ \forall n \in \{1,2\}$, as stipulated in the COP condition of (8), we can guarantee that the per user basis condition is also met. At the receiver, UAV-BS recover and merges each of these two split messages corresponding to each user separately to retrieve their original messages. Thus, the conditions described above, should be satisfied for each part of message separately. We can use the same justification for the SOP constraint (9).

$$\rho_{m,k,n}=\frac{p_{m,k,n}\left|\mathbf{w}_m^H\mathbf{h}_{m,k}\right|^2}{\sum\limits_{(k',n')\in\Phi_{m,k,n}}p_{m,k',n'}\left|\mathbf{w}_m^H\mathbf{h}_{m,k'}\right|^2+\sum\limits_{i=1,i\neq m}^{M}\sum\limits_{k''=1}^{K_i}P_{i,k''}\left|\mathbf{w}_m^H\mathbf{h}_{i,k''}\right|^2+\sigma_m^2} \tag{6}$$

$$=\frac{p_{m,k,n}\mathrm{PL}\left(d_{m,k}\right)\left|\mathbf{w}_m^H\mathbf{f}_{m,k}\right|^2}{\underbrace{\sum\limits_{(k',n')\in\Phi_{m,k,n}}p_{m,k',n'}\mathrm{PL}\left(d_{m,k'}\right)\left|\mathbf{w}_m^H\mathbf{f}_{m,k'}\right|^2}_{\mathrm{IUI}}+\underbrace{\sum\limits_{i=1,i\neq m}^{M}\sum\limits_{k''=1}^{K_i}P_{i,k''}\mathrm{PL}\left(d_{i,k''}\right)\left\|\sin\left(\phi_{i,k''}\right)\mathbf{f}_{i,k''}\right\|^2\left|\mathbf{w}_m^H\mathbf{e}_{i,k''}\right|^2}_{\mathrm{ICI}}+\sigma_m^2}$$

the discontinuous variable Φ_m, the problem in (10) represents a non-convex mixed integer programming problem. In the next section, we derive closed-form expressions both for the COP and SOP constraints, while Φ_m is obtained through an exhaustive search.

IV. ENST Maximization Solution

In this section, we construct the overall algorithm for finding the optimal solution of (10).

A. Handling the Probabilistic Constraints (10)-C_1 and (10)-C_2

We first intend to handle the COP constraint (10)-C_1 . In this regard, we first insert (6) into (8), (10)-C_1 can be reformulated as (11) , where $\beta_{m,n,k}=2^{r_{m,k,n}}-1$, $\lambda_{m,k',n'}\triangleq\frac{1}{2p_{m,k',n'}\mathrm{PL}\left(d_{m,k'}\right)}$, and $\lambda_{i,k''}=\frac{2^{\frac{B}{N_t-1}}}{P_{i,k''}\mathrm{PL}\left(d_{i,k''}\right)}$ (*Proof*: See Appendix A).

Upon inserting (7) into (9), we can reformulate the SOP constraint (10)-C_2 as (12), where $\eta_{j,k,n}=\frac{1}{p_{m,k,n}\mathrm{PL}(d_{m,k,j})\lambda_j^{max}\left\{\tilde{\mathbf{Q}}_{m,j}\right\}}$, $\zeta_{j,k',n'}=\frac{1}{p_{m,k',n'}\mathrm{PL}\left(d_{m,k',j}\right)\lambda_j^{max}\left\{\tilde{\mathbf{Q}}_{m,j}\right\}}$, and $\kappa_{j,k,n}=2^{D_{j,k,n}}-1$ (*Proof*: See Appendix B). On the other hand, as detailed in [37], since $D_{j,k,n}$ independent of both $r_{k,m,n}$ and $p_{k,m,n}$ within the OF, the maximization problem (10) over $D_{j,k,n}$ is equivalent to minimizing $D_{j,k,n}$. To find a more conservative solution, we exploit that $D_{j,k,n}$ appears both in the OF and in the SOP constraint (10), we have to exploit a tighter constraint than (12) for obtaining the minimum value of $D_{j,k,n}$, which is given by (13), where $W_0\left(x\right)$ is the Lambert W-function. However, it is still challenging to solve (10), since $r_{k,m,n}$ and $p_{k,m,n}$ are coupled in the OF of (10). To arrive at a more tractable form, the operations of maximization and the minimization can be swapped in (10). Additionally, since $\{D_{j,k,n}\}_{j=1}^{M}$ are independent, we can actually solve J independent maximization problems and then simply choose the minimum one. Furthermore, by exploiting the inequalities of $\exp\left(-x\right)\leq\frac{1}{1+x}$ and $\frac{1}{1+x}\leq\frac{1}{x}$, we can instead replace the lower bound and upper bound of the OF and of the COP constraint (10), respectively. Accordingly, based on what was mentioned above, a bound of the solution may be obtained as (14), where we have $A\triangleq|\Phi_{m,k,n}|+M+K_i$, $\xi\triangleq\prod\limits_{i=1,i\neq m}^{M}\prod\limits_{k''=1}^{K_i}2\lambda_{i,k''}^{-1}$.

Now, we can exploit the block coordinate decent technique, where $\{p_{m,k,1},D_{j,k,1},\ p_{m,k,2},D_{j,k,2}\}_{k=1}^{K_M}$ and the $\{r_{m,k,1},r_{m,k,2}\}_{k=1}^{K_M}$ are found successively in an iterative manner. In particular, the l^{th} iteration of the algorithm is constituted by separately maximizing the criterion with respect to each of $\{r_{m,k,1},r_{m,k,2}\}_{k=1}^{K_M}$ and $\{p_{m,k,1},D_{j,k,1},\ p_{m,k,2},D_{j,k,2}\}_{k=1}^{K_M}$, while keeping the other one fixed. Given this perspective, we first update $\{r_{m,k,1},r_{m,k,2}\}_{k=1}^{K_M}$, while assuming that $\{p_{m,k,1},D_{j,k,1},\ p_{m,k,2},D_{j,k,2}\}_{k=1}^{K_M}$ are fixed values which results in the following optimization problem:

$$\min_{1\leq j\leq J}\left(\max_{\{r_{m,k,1},r_{m,k,2}\}}\left\{\sum_{k=1}^{K_m}\sum_{n=1}^{2}\exp\left(\Xi_{m,n}^{r}\frac{\beta_{m,n,k}}{2}\right)r_{m,k,n}\right\}\right) \tag{15}$$

s.t.

$$C_1:\xi\exp\left(-\tfrac{\beta_{m,n,k}\sigma_m^2}{2}\right)\beta_{m,n,k}^{-A}\prod_{(k',n')\in\Phi_{m,k,n}}\left(2\lambda_{m,k',n'}^{*^{-1}}\right)\leq\epsilon_{cop},$$

$\forall\,k,n$, where $\Xi_{m,n}^{r}\triangleq\sum\limits_{(k',n')\in\Phi_{m,k,n}}\lambda_{m,k',n'}^{*^{-1}}+\xi-\sigma_m^2$.

It is easy to check that in terms of $\{r_{m,k,1},r_{m,k,2}\}_{k=1}^{K_M}$, while the OF of (15) is an increasing function, constraint (15)-C_1 is a decreasing one. Hence, the closed form expression of $\{r_{m,k,1},r_{m,k,2}\}_{k=1}^{K_M}$ may obtained when the inequality constraint (15)-C_1 is active at the optimum. Hence, the optimal point of (15), i.e., $\left\{r_{m,k,1}^{*},{r_{m,k,2}}^{*}\right\}_{k=1}^{K_M}$, may be found by solving the following equation:

$$\exp\left(-\frac{\sigma_m^2\beta_{m,n,k}}{2}\right)\beta_{m,n,k}^{-A}=\frac{\epsilon_{cop}}{\xi}\prod_{(k',n')\in\Phi_{m,k,n}}\left(\frac{\lambda_{m,k',n'}^{*}}{2}\right). \tag{16}$$

By doing so, followed by some algebraic manipulations, together with the help of the principal branch of the Lambert W-function, the optimum is formulated as follows:

$$r_{m,k,n}^{*}=\log_2\left(1+\frac{2A}{\sigma_m^2}W_0\left(\left[\xi{\epsilon_{cop}}^{-1}\prod_{(k',n')\in\Phi_{m,k,n}}\left(2\lambda_{m,k',n'}^{*^{-1}}\right)\right]^{\frac{1}{A}}\right)\right). \tag{17}$$

Now, assuming $\left\{r_{m,k,1}^{*},{r_{m,k,2}}^{*}\right\}_{k=1}^{K_m}$ to be fixed values, we can update $\{p_{m,k,1},D_{j,k,1},\ p_{m,k,2},D_{j,k,2}\}_{k=1}^{K_M}$, which result in the following equivalent transformation of (15) in the log-domain as (18), where $\mathcal{F}_j\triangleq\sum\limits_{k=1}^{K_m}\sum\limits_{n=1}^{2}\beta_{m,n,k}^{*}$

$$P_{m,k,n}^{CO} = 1 - \exp\left(-\frac{\beta_{m,n,k}\sigma_m^2}{2}\right) \prod_{(k',n')\in\Phi_{m,k,n}} \left(1+\lambda_{m,k',n'}^{-1}\frac{\beta_{m,n,k}}{2}\right)^{-1} \prod_{i=1,i\neq m}^{M}\prod_{k''=1}^{K_i}\left(1+\lambda_{i,k''}^{-1}\frac{\beta_{m,n,k}}{2}\right)^{-1}, \forall k\in\mathcal{K}_m \quad (11)$$

$$P_{j,k,n}^{SO} \triangleq \mathbb{P}\left\{D_{j,k,n} \leq \log_2\left(1+\mu_{j,k,n}\right)\right\} = \exp\left(-\eta_{j,k,n}\kappa_{j,k,n}\sigma_e^2\right) \prod_{(k',n')\neq(k,n)} \left(1+\eta_{j,k,n}\kappa_{j,k,n}\zeta_{j,k',n'}^{-1}\right)^{-1}, \quad (12)$$

$$D_{j,k,n} \geq \log_2\left(1+\frac{2K_m-1}{\eta_{j,k,n}\sigma_e^2} W_0\left(\frac{\eta_{j,k,n}\sigma_e^2}{2K_m-1}\left(\frac{\prod_{(k',n')\neq(k,n)}\zeta_{j,k',n'}}{\eta_{j,k,n}}\epsilon_{sop}{}^{-1}\right)^{\frac{1}{2K_m-1}}\right)\right), \quad (13)$$

$$\min_{1\leq j\leq J}\left(\max_{\mathcal{S}}\left\{\sum_{k=1}^{K_m}\sum_{n=1}^{2}\exp\left(\frac{\beta_{m,n,k}}{2}\left[\sum_{(k',n')\in\Phi_{m,k,n}}\lambda_{m,k',n'}^{-1}+\xi-\sigma_m^2\right]\right)\left[r_{m,k,n}-D_{j,k,n}\right]^+\right\}\right) \quad (14)$$

$$\text{s.t. } \xi\exp\left(-\tfrac{\beta_{m,n,k}\sigma_m^2}{2}\right)\beta_{m,n,k}^{-A}\prod_{(k',n')\in\Phi_{m,k,n}} 2\lambda_{m,k',n'}^{-1} \leq \epsilon_{cop},\ \ \forall k,n,\ \ C_2:(13),\ \ C_3:(10\text{-}C_3)$$

$\left[\sum_{(k',n')\in\Phi_{m,k,n}} \mathrm{PL}\left(d_{m,k'}\right)p_{m,k',n'}\right] + \ln\left[r_{m,k,n}^{*}-D_{j,k,n}\right]$, $\gamma \triangleq 2^{-2|\Phi_{m,k,n}|}\ \epsilon_{cop}\xi^{-1}\ \exp\left(\frac{\beta_{m,n,k}^{*}\sigma_m^2}{2}\right)\ \beta_{m,n,k}^{*\left(|\Phi_{m,k,n}|+M+K_i\right)}$, and $\psi_k \triangleq \log_2(\gamma) - \sum_{(k',n')\in\Phi_{m,k,n}} \log_2\left(\mathrm{PL}\left(d_{m,k'}\right)\right)$.

Note that the newly added constraint (18)-C_3 arises from the fact that the point-wise maximum operator $[]^+$ within the OF of (14) leads to non-convexity. Thus, by adding (18)-C_3 we are equivalently stating that the OF must be non-negative at the optimum and then we can simply remove $[]^+$. Now, since the OF in (18) is constituted by the sum of convex and affine functions with respect to $\{p_{m,k,1}, D_{j,k,1},\ p_{m,k,2}, D_{j,k,2}\}_{k=1}^{K_M}$, it is a convex function. However, problem (18) is still non-convex because of the non-convex constraint (18)-C_2 . To circumvent the non-convexity, we harness the SPCA of [5], [18], where the non-convex factor is approximated by its first-order Taylor expansion at each iteration. Given this perspective, in the following we attempt to circumvent the non-convexity imposed by the fractional form and the logarithmic function within (18)-C_2 by introducing some auxiliary variables, namely $\{\theta_{j,k,n}, \varrho_{j,k,n}, \nu_{j,k,n}, \vartheta_{j,k,n}\}$. Following the classic variable transformation approach, the constraint (18)-C_2 can be decomposed into $\forall k,j,n$,:

$$D_{j,k,n} \geq \log_2\left(1+\theta_{j,k,n}\right),\ \forall k,j,n, \quad (19)$$

$$\theta_{j,k,n} \leq \frac{\mathrm{PL}\left(d_{m,k,j}\right)\left(2K_m-1\right)}{\sigma_e^2} p_{m,k,n}\varrho_{j,k,n}, \quad (20)$$

$$\varrho_{j,k,n} \leq W_0\left(\nu_{j,k,n}\right), \quad (21)$$

$$\nu_{j,k,n}p_{m,k,n}^{2K_m} \leq \frac{\sigma_e^2}{\mathrm{PL}\left(d_{m,k,j}\right)^{2K_m}\left(2K_m-1\right)}\vartheta_{j,k,n}, \quad (22)$$

$$\vartheta_{j,k,n} \leq \left(\prod_{(k',n')\neq(k,n)}\zeta_{j,k',n'}\epsilon_{sop}{}^{-1}\right)^{\frac{1}{2K_m-1}}. \quad (23)$$

Now, since the non-convexity still persists within (19)-(23), we attempt to approximate the non-convex factor at each iteration by its first-order Taylor expansion at the t^{st} SPCA iteration. Following this approach, the affine approximation becomes straightforward for each of (19)-(23). Hence , we can replace each non-convex constraint by its affine approximation, and thus the equivalent convex form of (18)-C_2 at the t^{st} SPCA iteration may be formulated as:

$$g_1(\mathbf{x}) \triangleq 1+\theta_{j,k,n} - \Gamma^{[t]}\left(D_{j,k,n}\right) \leq 0, \quad (24)$$

$$g_2(\mathbf{x}) \triangleq \theta_{j,k,n} - \frac{\mathrm{PL}\left(d_{m,k,j}\right)\left(2K_m-1\right)}{\sigma_e^2}\Theta^{[t]}\left(p_{m,k,n},\varrho_{j,k,n}\right) \leq 0, \quad (25)$$

$$g_3(\mathbf{x}) \triangleq \varrho_{j,k,n} - W_0\left(\nu_{j,k,n}^{[t]}\right)\left(\nu_{j,k,n}^{[t]}\left(1-W_0\left(\nu_{j,k,n}^{[t]}\right)\right)\right)^{-1} \times\left(\nu_{j,k,n}-\nu_{j,k,n}^{[t]}\right) \leq 0, \quad (26)$$

$$g_4(\mathbf{x}) \triangleq \Psi^{[t]}\left(\nu_{j,k,n},p_{m,k,n}^{2K_m}\right) - \frac{\sigma_e^2}{\mathrm{PL}\left(d_{m,k,j}\right)^{2K_m}\left(2K_m-1\right)}\vartheta_{j,k,n} \leq 0, \quad (27)$$

$$g_5(\mathbf{x}) \triangleq \Lambda^{[t]}\left(\vartheta_{j,k,n}\right) - \frac{\left(\sum_{(k',n')\neq(k,n)}\log\left(\zeta_{j,k',n'}\right)-\log\left(\epsilon_{sop}\right)\right)}{\left(2K_m-1\right)} \leq 0, \quad (28)$$

$\forall k,j,n$, respectively, $\Theta^{[t]}\left(p_{m,k,n},\varrho_{j,k,n}\right) \triangleq \frac{1}{4}\left(p_{m,k,n}+\varrho_{j,k,n}\right)^2 + \frac{1}{4}\left(p_{m,k,n}^{[t]}-\varrho_{j,k,n}^{[t]}\right)^2 - \frac{1}{2}\left(p_{m,k,n}^{[t]}-\varrho_{j,k,n}^{[t]}\right)\left(p_{m,k,n}-\varrho_{j,k,n}\right)$, $\Gamma^{[m]}\left(D_{j,k,n}\right) \triangleq 2^{D_{j,k,n}^{[t]}}\left[1+\ln(2)\left(D_{j,k,n}-D_{j,k,n}^{[t]}\right)\right]$, $\Lambda^{[t]}\left(\zeta_{j,k',n'}\right) \triangleq \log\left(\zeta_{j,k',n'}^{[t]}\right) + \frac{\zeta_{j,k',n'}-\zeta_{j,k',n'}^{[t]}}{\zeta_{j,k',n'}^{[t]}}$, and $\Psi^{[t]}\left(\nu_{j,k,n},p_{m,k,n}^{2K_m}\right) \triangleq \nu_{j,k,n}^{[t]}\left(p_{m,k,n}^{[t]}\right)^{2K_m} + \left(p_{m,k,n}^{[t]}\right)^{(2K_m-1)}\left[\left(p_{m,k,n}^{[t]}\right),\ (2K_m-1)\ \nu_{j,k,n}^{[t]}\right] \times \left[\nu_{j,k,n}-\nu_{j,k,n}^{[t]},\ p_{m,k,n}-p_{m,k,n}^{[t]}\right]^T$.

In order to arrive at (26) from (21), we have exploited the fact that since $W_0(x)$ is concave over the interval of

$$\min_{1\le j\le J}\left(\max_{\left\{p_{m,k,1},D_{j,k,1},\ p_{m,k,2},D_{j,k,2}\right\}_{k=1}^{K_M}}\{\mathcal{F}_j\}\right), \tag{18}$$

s.t. $C_1:\sum_{(k',n')\in\Phi_{m,k,n}}\log_2\left(p_{m,k',n'}\right)\le\psi_k,\ C_2:(13),\ C_3:r^*_{m,k,n}\ge D_{j,k,n}, C_4:\sum_{n=1}^{2}p_{m,k,n}\le P_{m,k},\ p_{m,k,n}\ge 0,$

$$\min_{1\le j\le J}\left(\max_{\mathbf{X}}\{\mathcal{F}_j\}\right), \tag{29}$$

s.t. (18-C_1, C_3, C_4),(24) (25), (26), (27), (28)

Algorithm 1 : Proposed secure resource allocation

For $\Phi_m\in\mathbf{\Pi}_m$ do:
Call **Function** *Outer_Loop*
End.
Obtain the optimal solution $\left\{p^*_{m,k,1},D^*_{j,k,1},p^*_{m,k,2},D^*_{j,k,2}\right\}_{k=1}^{K_m}$, $\left\{r^*_{m,k,1},r^*_{m,k,2}\right\}_{k=1}^{K_m}$ and optimal decoding order Φ^*_m=Φ_m with the highest OF.
Function *Outer_Loop*
Step 1: Initialize the maximum number of iterations Q_{max}, T_{max} and the maximum tolerance ϵ.
Step 2: Initialize $\left\{{r^*_{m,k,1}}^{[0]},{r^*_{m,k,2}}^{[0]}\right\}$ and the outer iteration index $q=0$.
While $\left(\left|{r^*_{m,k,n}}^{[q+1]}-{r^*_{m,k,n}}^{[q]}\right|\ge\epsilon \text{ or } q\le Q_{max}\right)\ \forall k,n$, do:
Step 3: Call the **Function** *Inner_Loop* with $\left\{{r^*_{m,k,1}}^{[q]},{r^*_{m,k,2}}^{[q]}\right\}$ to obtain the ϵ-constraint solution $\left\{p^*_{m,k,1},D^*_{j,k,1},p^*_{m,k,2},D^*_{j,k,2}\right\}$.
Step 4: Update ${r^*_{m,k,n}}^{[q+1]}$ in (17).
Step 5: **Goto** Step 3.
end while.
Step 6: Return the ϵ-constraint solution $\left\{p^*_{m,k,1},D^*_{j,k,1},p^*_{m,k,2},D^*_{j,k,2}\right\}$, $r^*_{m,k,1}={r^*_{m,k,1}}^{[q+1]}$ and $r^*_{m,k,2}={r^*_{m,k,2}}^{[q+1]}$.
end.
Function *Inner_Loop* $\left(\left\{{r^*_{m,k,1}}^{[q+1]},{r^*_{m,k,2}}^{[q+1]}\right\}\right)$
Step 1: Initialize the inner iteration index $t=0$, $\left\{p^{[0]}_{m,k,1},D^{[0]}_{j,k,1},p^{[0]}_{m,k,2},D^{[0]}_{j,k,2}\right\}$.
While $\left(\left|\mathcal{F}_j^{[t+1]}-\mathcal{F}_j^{[t]}\right|\ge\delta_I \text{ or } t\le T_{max}\right)$ do:
Step 2: Find the ϵ-constraint solution $\left\{p^{[t+1]}_{m,k,1},D^{[t+1]}_{j,k,1},p^{[t+1]}_{m,k,2},D^{[t+1]}_{j,k,2}\right\}$ of the following problem for given $\left\{p^{[t]}_{m,k,1},D^{[t]}_{j,k,1},p^{[t]}_{m,k,2},D^{[t]}_{j,k,2}\right\}$, and ${r^*_{m,k,n}}^{[m]}$
$\left\{p^{[t+1]}_{m,k,1},D^{[t+1]}_{j,k,1},p^{[t+1]}_{m,k,2},D^{[t+1]}_{j,k,2}\right\}=$ Solving (29),
Step 3: Update $\mathcal{F}_j^{[t+1]}$.
Step 4: **Goto** Step 2.
end while.
Step 5: Return $\left\{p^*_{m,k,1},D^*_{j,k,1},p^*_{m,k,2},D^*_{j,k,2}\right\}=\left\{p^{[t+1]}_{m,k,1},D^{[t+1]}_{j,k,1},p^{[t+1]}_{m,k,2},D^{[t+1]}_{j,k,2}\right\}$.
end

$\left(-e^{-1},\infty\right)$ and positive over $(1,\infty)$, upon using the first order Taylor expansion of $W_0(x)$ we have $W_0(\nu_{j,k,n})\le W_0\left(\nu^{[t]}_{j,k,n}\right)\left[\nu^{[t]}_{j,k,n}\left(1-W_0\left(\nu^{[t]}_{j,k,n}\right)\right)\right]^{-1}\left(\nu_{j,k,n}-\nu^{[t]}_{j,k,n}\right)$.

B. Overall Solution of the Original Problem (10)

Note that due to the decoding order constraint $\{\Phi_m\}$, it is challenging to find the optimal solution of problem (10). To solve this problem, we first fix the decoding order Φ_m to obtain the optimal triplet $\left\{r^*_{k,m,n}\ge 0,\ D^*_{j,k,n}\ge 0,\ p^*_{m,k,n}\ge 0\right\}$ and then exhaustively search the entire set to find the optimal Φ^*_m[7]. Upon assuming a fixed Φ_m, we conceive a two-tier iterative algorithm for attaining the overall ϵ-constraint solution $\left\{p^*_{m,k,1},D^*_{j,k,1},p^*_{m,k,2},D^*_{j,k,2}\right\}$ in two different tiers. More explicitly, using the approximations obtained in (24)-(28), together with $\left\{r^*_{k,m,1},r^*_{k,m,2}\right\}$ gleaned from the outer tier, the $(t+1)^{st}$ iteration of the inner tier solves the following equivalent convex form of problem (18) for finding the ϵ-constraint solution as (29), where $\mathbf{X}\triangleq\left(\boldsymbol{x},\{p_{m,k,1},D_{j,k,1},\ p_{m,k,2},D_{j,k,2}\}_{k=1}^{K_M}\right)$, and $\boldsymbol{x}\triangleq\{\theta_{j,k,n},\varrho_{j,k,n},\nu_{j,k,n},\vartheta_{j,k,n},\nu_{j,k,n}\}$. Upon the ϵ-constraint point $\left\{p^*_{m,k,1},D^*_{j,k,1},p^*_{m,k,2},D^*_{j,k,2}\right\}$ found by the inner loop, the $(q+1)^{st}$ iteration of the outer loop finds ϵ-constraint solution $\left\{{r^*_{m,k,1}}^{[q+1]},{r^*_{m,k,2}}^{[q+1]}\right\}$, given by (30), where the superscript "$*$" represents the final iteration of the inner loop. Since the proposed method consists of two layers of iterations, the stopping criterion of each layer depends on the relative change of the two consecutive of values. Therefore, the outer loop proceeds to the next iteration and runs until $\left|{r^*_{m,k,n}}^{[q+1]}-{r^*_{m,k,n}}^{[q]}\right|\le\epsilon$ is met or the maximum affordable number of iterations Q_{max} is reached. To find the ϵ-constraint solution $\left\{p^*_{m,k,1},p^*_{m,k,2},D^*_{j,k,n}\right\}$, the problem ((29)) is solved using the classic SPCA in another iterative process of the inner loop. In particular, the inner iterations are continued until the stopping criterion of $\left|\mathcal{F}_j^{[t+1]}-\mathcal{F}_j^{[t]}\right|\le\delta_I$[8] is satisfied at the $(t+1)^{st}$ iteration or the maximum affordable number of iterations T_{max} is reached. The proposed two-tier

[7]Although it would also be beneficial to look for an optimal SIC-ordering [5], [6], as the UAV is assumed to only have access to the AoA and distances, but not to the small-scale fading parameters, we have not performed the SIC-ordering here and left it for future works. It has been shown in [5] that for an algorithm including N initial points, the exhaustive SIC ordering for a K users uplink-RSMA imposes a tolerable computational complexity of $\mathcal{O}\left(2^K+NK^3\left(2K!\right)/2^K\right)$.

[8]Note that $\mathcal{F}_j^{[t]}$ represents the value of $\mathcal{F}_j$ at iteration t^{th} .

$$\underset{\text{obtained from (29)}}{\left\{p^*_{m,k,1}, D^*_{j,k,1}, p^*_{m,k,2}, D^*_{j,k,2}\right\}} \Leftrightarrow {r^*_{m,k,n}}^{[q+1]} = \log_2\left(1+\frac{2A}{\sigma_m^2}W_0\left(\left[\xi\epsilon_{cop}{}^{-1}\prod_{(k',n')\in\Phi_{m,k,n}}\left(2\lambda^{*-1}_{m,k',n'}\right)\right]^{\frac{1}{A}}\right)\right), \tag{30}$$

scheme is presented in Algorithm I[9].

V. Complexity and Convergence Analysis

A. Computational Complexity Analysis

In the proposed method, the computational complexity is dominated by solving problem (29). According to Algorithm 1, a solution of problem (29) is obtained via solving a series of convex problems with different initial points and decoding order strategies. Considering that the dimension of the variables in problem (29) is $\mathcal{L}_m = 5(1+J)K_m$, the worst-case complexity order of solving the convex problem in Step 2 of the inner-loop by using the standard interior point method is given by $\mathcal{O}\left(\left(\frac{\mathcal{L}_m-1}{2}\right)^3\right)$ [39, Pages 487, 569]. Since each cluster consists of K_m users and each user transmits a superposition of two messages (i.e., there are $2K_m$ messages for the m^{th} cluster), the decoding order set $\mathbf{\Pi}_m$ consists of $\frac{(2K_m)!}{2^{K_m}}$ elements. Therefore, the total complexity of solving problem (29) at each iteration is given by $\mathcal{O}\left(\left(\frac{\mathcal{L}_m-1}{2}\right)^3\frac{(2K_m)!}{2^{K_m}}\right)$. In practice, we consider small K_m to reduce the SIC complexity, so that the computational complexity of Algorithm 1 remains practical. To deal with a large number of users, we can increase the number of clusters and the users can be classified into different clusters, each having a small number of users.

B. Convergence Analysis

In this section we provide the convergence analysis of the SPCA algorithm. Since the original problem (14) is non-convex, it is not possible to prove convergence to a global minimum, but convergence to KKT points under some regularity conditions may be shown. The following lemmas will be used in the convergence proof. For simplicity we define $\Omega \triangleq$ feasible set of (14), $\Omega^{[t]} \triangleq$ feasible set of (29) for the t^{th} iteration.

Lemma 1. *Let $\mathcal{D} : \mathbb{R}^n \to \mathbb{R}$ be a strictly convex and differentiable function on a nonempty convex set $S \subseteq \mathbb{R}^n$. Then $\mathcal{D}$ is strongly convex on the set S. (Proof: See [38]).*

Lemma 2. *Assume that $\left\{\mathbf{X}^{[t]}\right\}$ is a sequence generated by the SPCA method. Then, for every $t \geq 0$: **i).** $\Omega^{[t]} \subseteq \Omega$, **ii).** $\mathbf{x}^{[t]} \in \Omega^{[t]} \cap \Omega^{[t+1]}$, **iii).** $\mathbf{X}^{[t]}$ is a feasible point of* (14)*, **iv).** $\mathcal{F}_j^{[t+1]} \leq \mathcal{F}_j^{[t]}$. (Proof: See [38]).*

Lemma 3. *The sequence $\left\{\mathcal{F}_j^{[t]}\right\}$ converges. (Proof: See [38]).*

[9]Note that if Algorithm 1 is initialized with random points, it may fail at the very beginning, because of infeasibility. To circumvent this issue, we now conceive a feasible initial point search algorithm (FIPSA). This approach has been proposed in [5], [18] as a low-complexity scheme for finding the feasible initial points.

Recall that a feasible solution $\mathbf{X}^*$ of an optimization problem is *regular*, if the set of gradients of the active constraints at $\mathbf{X}^*$ is linearly independent [39]. If $\mathbf{X}^{[t]}$ converges to a regular point $\mathbf{X}^*$, then $\mathbf{X}^*$ is a KKT point of problem (14). By Lemma 2 it follows that the strictly convex objective function $\mathcal{F}_j$ is also strongly convex on the convex feasible set $\Omega^{[t+1]}$. In particular, there exists a $\vartheta > 0$ such that $\forall k \geq 0$, we have:

$$\mathcal{F}_j^{[t]} - \mathcal{F}_j^{[t+1]} \geq \left(\mathbf{X}^{[t]} - \mathbf{X}^{[t+1]}\right)^{\mathrm{T}} \nabla\mathcal{F}_j^{[t+1]} + \vartheta\left\|\mathbf{X}^{[t]} - \mathbf{X}^{[t+1]}\right\|^2, \tag{31}$$

since $\mathbf{X}^{[t]}$ is a feasible point of (29) (by Lemma 3), and $\mathbf{X}^{[t+1]}$ is its optimum. Then from the optimality conditions of the $(t+1)^{th}$ iteration of (29) (see [40, proposition 2.1.2]), we obtain $\left(\mathbf{X}^{[t]} - \mathbf{X}^{[t+1]}\right)^{\mathrm{T}} \nabla\mathcal{F}_j^{[t+1]} \geq 0$, which combined with (31) yields:

$$\mathcal{F}_j^{[t]} - \mathcal{F}_j^{[t+1]} \geq \vartheta\left\|\mathbf{X}^{[t]} - \mathbf{X}^{[t+1]}\right\|^2. \tag{32}$$

By Lemma 3, the sequence $\left\{\mathcal{F}_j^{[t]}\right\}$ converges and thus the inequality (32) implies that $\left\|\mathbf{X}^{[t]} - \mathbf{X}^{[t+1]}\right\| \to 0$. Let $\mathbf{X}^\diamondsuit \triangleq \left(\boldsymbol{x}^\diamondsuit, \left\{p^\diamondsuit_{m,k,1}, D^\diamondsuit_{j,k,1}, p^\diamondsuit_{m,k,2}, D^\diamondsuit_{j,k,2}\right\}_{k=1}^{K_M}\right)$ be an accumulation point of the sequence $\left\{\mathbf{X}^{[t]}\right\}$. Then we will show that $\mathbf{X}^\diamondsuit$ is a KKT point. Since $\mathbf{X}^\diamondsuit$ is an accumulation point of $\left\{\mathbf{X}^{[t]}\right\}$, there exists a subsequence $\left\{\mathbf{X}^{[t_n]}\right\}$ such that $\mathbf{X}^{[t_n]} \to \mathbf{X}^\diamondsuit$, when the number of iteration $n \to \infty$. Regarding the limit point $\mathbf{X}^\diamondsuit$, we can make the following statement.

Corollary 4. *The accumulation point $\mathbf{X}^\diamondsuit$ of the sequence $\left\{\mathbf{X}^{[t]}\right\}$ generated by the proposed SPCA method is a KKT point of* (29)*.*

Proof: We know from [39] that there exist Lagrangian multipliers λ_i^* together with the accumulation point $\mathbf{X}^\diamondsuit$ that satisfy the following KKT's necessary and sufficient condition for the optimality of convex problems [39, Sec 5.5], where $\{\gamma_i\}_{i=1}^8$ in (33) denote the Lagrangian multiplies of problem (29). If we choose $\gamma_i = \lambda_i$ for $i = 1, ..., 8$, we conclude that the point $\mathbf{X}^\diamondsuit$ also satisfy. Hence, we proved that if the sequence $\left\{\mathbf{X}^{[t]}\right\}$ generated by the SPCA method converges to a regular point $\mathbf{X}^\diamondsuit$, then $\mathbf{X}^\diamondsuit$ is a KKT point of the SPCA problem (29). It has already been shown that the point $\mathbf{X}^\diamondsuit$ is a KKT point (stationary point) of the SPCA problem (29). This stationary point cannot be a saddle point, since the objective function $\mathcal{F}_j$ is strictly convex and twice-continuously differentiable in the variable $\mathbf{X}$. By the contradiction method, we can also show that the point $\mathbf{X}$ cannot be a local maximum [39].

■

$$\nabla \mathcal{F}_j + \gamma_1 \nabla \left(\sum_{(k',n') \in \Phi_{m,k,n}} \log_2 \left(p_{m,k',n'} \right) - \psi_k \right) + \gamma_2 \nabla g_1(\mathbf{x}) + \gamma_3 \nabla g_2(\mathbf{x}) + \Theta^{[t]} \left(p_{m,k,n}, \varrho_{j,k,n} \right) - \theta_{j,k,n} \Bigg) + \gamma_4 \nabla g_3(\mathbf{x}) +$$

$$\gamma_5 \nabla g_4(\mathbf{x}) + \gamma_6 \nabla \left(D_{j,k,n} - r^*_{m,k,n} \right) + \gamma_7 \nabla g_6(\mathbf{x}) + \gamma_8 \nabla \left(\sum_{n=1}^{2} p_{m,k,n} - P_{m,k} \right) = 0. \tag{33}$$

VI. Simulation Results

In this section, we evaluate the secure transmission performance of the proposed algorithm through simulations. Each point in the figures is obtained by averaging over 150 simulation trials. Unless otherwise specified, the simulation setup is as follows throughout this section. In the scenario investigated a UAV hovers above the users to provide communication services. Explicitly, the UAV has a coverage radius of $R_{UAV} = 800\,\text{m}$ and altitude of $H_i = 140\,\text{m}$. The path-loss model in the UAV network includes both LoS and non-LoS links associated with the path-loss exponents of $\mathcal{L}_{m,k} = 2$ and $\mathcal{N}_{m,k} = 3.5$, respectively. There are $M = 3$ clusters, 100 users associated with $P_{i,k} = \frac{P}{\sum_{m=1}^{M} K_m}$, where P is the total power budget, and $J = 3$ Eves randomly distributed in the whole system between 1 m and 800 m. Once the large-scale fading parameters are generated, they are assumed to be known and fixed throughout the simulations. The small-scale fading vectors of all users and Eves are independently generated according to $\mathcal{CN}(0, \mathbf{I}_{N_t})$. The noise power at each user and eavesdropper is set to $\sigma_m^2 = \sigma_e^2 = 0\,\text{dB}$. Moreover, we set $T_{max} = Q_{max} = 20$, $N_t = 5$, $\epsilon_{cop} = \epsilon_{sop} = 0.1$, and the maximum threshold value used for the termination of Algorithm 1 to $\delta_I = 10^{-2}$. The maximum tolerance of $\epsilon = 10^{-3}$ is assumed for the termination criterion used in Algorithm 1.

Firstly, in Fig. 3 we demonstrate the convergence of Algorithm 1 in solving (17) and (18) for different values of P. The convergence of the inner loop of Algorithm 1 in terms of updating $\mathcal{F}_j^{[t]}$ is shown by black-lines. It is observed that the inner loop converges within 6 iterations for different values of P, which corroborates the convergence of (29). When fixing the number of users, the power $P_{i,k}$ allocated to each user increases upon increasing P. As a result, the OF value of $\mathcal{F}_j^{[t]}$ in (29) increases as P increases. On the other hand, the convergence of the outer loop of Algorithm 1 is characterized by the red-lines. Observe that the algorithm used for solving (17) converges after a maximum of 10 iterations under different values of P. Fig. 4 shows the ENST of the proposed scheme versus J for different values of ϵ_{cop}. Naturally, upon increasing J, the performance degrades due to having more $Eves$ in the system, but using a higher ϵ_{cop} would increase ENST and compensate for the performance loss. Additionally, as another important observation, without performing SIC at *Eve* (ESIC), the *Eve*'s rate is decreased, resulting in ENST enhancement.

To show the performance advantages of the proposed scheme by employing the RSMA scheme, we compare it to both power-domain (PD) NOMA and TDMA. In PD-NOMA, the UAV first decodes the messages of users having high channel gains and then decodes the messages of users with low channel gains by subtracting the interference imposed by the previously decoded high-gain user. In TDMA, each user will be assigned a fraction of time to use the whole bandwidth. Let $\alpha_{m,k} = \frac{1}{K_m}$ be the fraction of time allocated to $U_{m,k}$. Then the data rate of $U_{m,k}$ becomes $C_{m,k}^{TDMA} = \alpha_{m,k} \log_2 \left(1 + \frac{p_{m,k,n} \left| \mathbf{w}_m^H \mathbf{h}_{m,k} \right|^2}{\sigma_m^2} \right)$. Observe from Fig. 5 that RSMA always achieves a better performance than PD-NOMA and TDMA. Moreover, the ENST gain of the proposed scheme over TDMA becomes more prominent as P and ϵ_{cop} increases.

The corresponding ENST versus ϵ plot is provided in Fig. 6, where the proposed scheme achieves a significantly higher ENST upon increasing P, ϵ_{sop} and ϵ_{cop}. A heuristic explanation of this phenomenon is that increasing both the connection and secrecy outage threshold tends to relax the constraints of (29), and decrease the lower bound of (18)-C_2, which in turn increases the ENST.

Finally, to show the importance of considering SIC ordering as well as imperfect CSIT, we compare the proposed scheme for both optimal SIC (OSIC) and Sub-optimal SIC (SSIC) ordering. Additionally, we also consider RSMA with perfect CSIT. To make a fair comparison, we simulate all schemes under the same security requirement. The ENST versus P trends recorded for different values of ϵ_{cop} are provided in Fig. 7, where the proposed scheme always achieves significantly higher ENST than RSMA ignoring CSIT uncertainty. Fig. 7 suggests that using bigger ϵ_{cop} would increase the ENST and mitigate the performance loss of SSIC.

Finally, Fig. 9 illustrates the ENST versus N_e. This figure indicates that increasing the number of the receive antennas at Eve, the system's secrecy performance is degraded due to Eve's improved ability to eavesdrop and infer from common message. Interestingly, our proposed scheme still shows considerable robustness against a multiple antenna-aided Eve, hence we can achieve non-zero ENST.

VII. Conclusions

In this article, we proposed secure RSMA uplink transmission under imperfect CSIT for a UAV-BS network, in which RSMA is employed by each legitimate users for secure transmission under large-scale uplink access. To characterize the performance of this system, an efficient block coordinate decent algorithm was proposed for maximizing the effective network secrecy throughput under the constraints of secrecy and the reliability outage probabilities and transmit power budget constraints. To solve this problem, we derived the closed-form optimal RS rate expression of each user. Then,

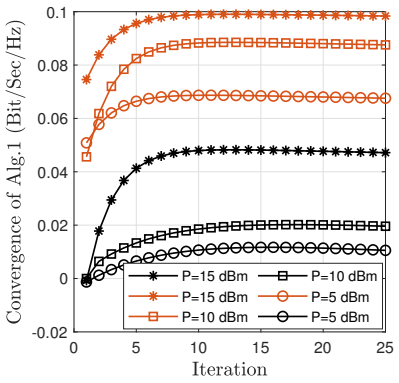

Fig. 3. The Convergence of Algorithm 1, black-line refer to $\mathcal{F}_j^{[t]}$ and red-line refer to ${r^*_{m,k,n}}^{[q]}$ for different values of P.

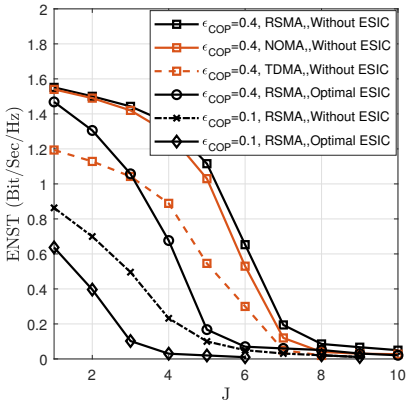

Fig. 4. ENST versus J for different values of ϵ_{cop} and with/without optimal Eve SIC ordering.

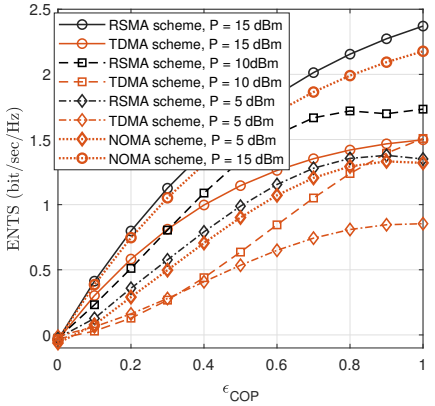

Fig. 5. ENST versus ϵ_{cop} for different values of P.

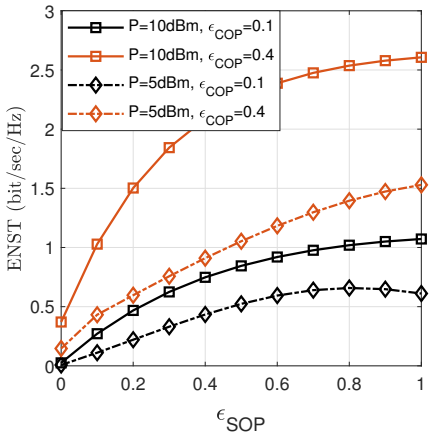

Fig. 6. ENST versus ϵ_{sop} for different values of P and ϵ_{cop}.

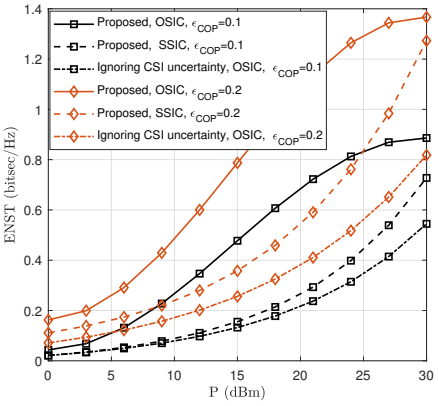

Fig. 7. ENST versus P for different values of ϵ_{cop} and SIC method.

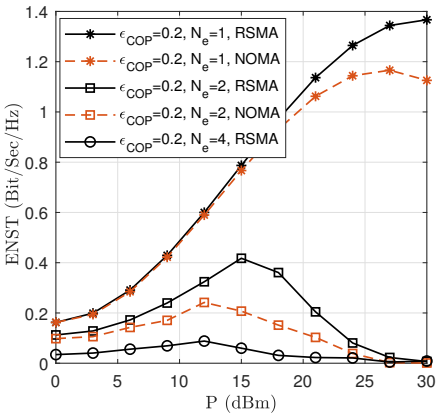

Fig. 8. ENST versus ϵ_{cop} for different values of N_e.

the ϵ-constraint transmit power of each user was calculated by the classic SPCA technique under a given decoding order and then the optimal decoding order was found by an exhaustive search method. Numerical results demonstrated that the proposed algorithm significantly improves the effective network secrecy throughput compared to the PD-NOMA and TDMA benchmarks, as well as to the RSMA transmission ignoring CSIT uncertainty.

APPENDIX A
DERIVATION OF (11)

Based on (8), $P^{CO}_{m,k,n}$ can be expressed as $A1$, where we have $\mathcal{X}_k \triangleq \left|\mathbf{w}_m^H \mathbf{f}_{m,k}\right|^2 \geq 0$, $\mathcal{Y}_{i,k''} \triangleq \|\mathbf{f}_{i,k''}\|^2 \sin^2(\phi_{i,k''}) \left|\mathbf{w}_m^H \mathbf{e}_{i,k''}\right|^2 \geq 0$. Otherwise, $P^{CO}_{m,k}$ is always one. Furthermore, based on the independence of the interference terms [7, eq 24], the variables $\{\mathcal{X}_k\}$ and $\{\mathcal{Y}_{i,k''}\}$ $\forall i,k,k''$ are indeed independent.

To obtain a closed-form expression of $P^{CO}_{m,k}$, we first provide the probability density function (pdf) of $\mathcal{X}_k$. Recall that $\mathbf{n}_{m,k} \sim \mathcal{CN}(0, \mathbf{I}_{N_t})$ and $\widetilde{\mathbf{f}}_{m,k} \triangleq \frac{\mathbf{f}_{m,k}}{\|\mathbf{f}_{m,k}\|}$, $\mathcal{X}_k$ can be rewritten as $\mathcal{X}_k = \|\mathbf{f}_{m,k}\|^2 \left|\mathbf{w}_m^H \widetilde{\mathbf{f}}_{m,k}\right|^2$. Since the normalized beamformer weights $\mathbf{w}_m$ are determined by $\{\mathbf{v}_i\}_{i=1,i\neq m}^{M}$ according to $\mathbf{w}_m^H \mathbf{v}_l = 0, \forall l \neq m$, and $\{\mathbf{v}_i\}_{i=1,i\neq m}^{M}$ are independent of $\mathbf{f}_{m,k}$, the vectors $\mathbf{f}_{m,k}$ and $\mathbf{w}_m$ are also independent. As a result, $\mathbf{f}_{m,k}$ and $\mathbf{w}_m$ are independent unit-norm vectors in the N_t-dimensional space. Based on [31, Lemma 1], the square inner product between two independent unit-norm random vectors is Beta distributed with shape parameters of $(1, N_t - 1)$, i.e., we have $X_1 \triangleq \left|\mathbf{w}_m^H \widetilde{\mathbf{f}}_{m,k}\right|^2 \sim \text{Beta}\,(1, N_t - 1)$ and its pdf is $f_{X_1}(x_1) = \frac{(1-x_1)^{N_t-2}}{\text{Be}(1,N_t-1)}$, $x_1 \in [0,1]$ [34, eq 8.380]. On the other hand, since we have $\mathbf{f}_{m,k} \sim \mathcal{CN}(0, \mathbf{I}_{N_t})$, $X_2 \triangleq \|\mathbf{f}_{m,k}\|^2$ is distributed as a chi-squared r.v. with $2N_t$ degrees of freedom as $\chi^2_{2N_t}$, and its pdf is $f_{X_2}(x_2) = \frac{x_2^{N_t-1} e^{-\frac{x_2}{2}}}{2^{N_t}\Gamma(N_t)}$, $x_2 \geq 0$, where $\Gamma(x)$ is the Gamma function [50, eq. 8.310]. Since $\mathcal{X}_k = X_1 X_2$, and X_1 and X_2 are independent, the pdf of $\mathcal{X}_k$ is given by:

$$f_{\mathcal{X}_k}(x) = \int_x \frac{1}{|x_2|} f_{X_2}(x_2) f_{X_1}\left(\frac{x}{x_2}\right) dx_2$$
$$= \frac{\int_x^{+\infty} (x_2 - x)^{N_t-2} e^{-\frac{x_2}{2}} dx_2}{\text{Be}\,(1, N_t - 1)\, 2^{N_t} \Gamma(N_t)} = \text{Exp}(\frac{1}{2}). \qquad (A2)$$

Thus, $\mathcal{X}_k \sim \text{Exp}(\frac{1}{2})$ is exponentially distributed with rate

$$\mathbb{P}\left\{2^{r_{m,k,n}}-1>\frac{p_{m,k,n}\mathrm{PL}\left(d_{m,k}\right)\left|\mathbf{w}_m^H\mathbf{f}_{m,k}\right|^2}{\sum_{(k',n')\in\Phi_{m,k,n}}p_{m,k',n'}\mathrm{PL}\left(d_{m,k'}\right)\left|\mathbf{w}_m^H\mathbf{f}_{m,k'}\right|^2+\sum_{i=1,i\neq m}^{M}\sum_{k''=1}^{K_i}P_{i,k''}\mathrm{PL}\left(d_{i,k''}\right)\left\|\sin\left(\phi_{i,k''}\right)\mathbf{f}_{i,k''}\right\|^2\left|\mathbf{w}_m^H\mathbf{e}_{i,k''}\right|^2+\sigma_m^2}\right\}$$
$$=\mathbb{P}\left\{2^{r_{m,k,n}}-1>\frac{p_{m,k,n}\mathrm{PL}\left(d_{m,k}\right)\mathcal{X}_k}{\sum_{(k',n')\in\Phi_{m,k,n}}p_{m,k',n'}\mathrm{PL}\left(d_{m,k'}\right)\mathcal{X}_{k'}+\sum_{i=1,i\neq m}^{M}\sum_{k''=1}^{K_i}P_{i,k''}\mathrm{PL}\left(d_{i,k''}\right)\mathcal{Y}_{i,k''}+\sigma_m^2}\right\}, \quad (A1)$$

$\lambda_k=\frac{1}{2}$. Now, we derive the pdf of $\mathcal{Y}_{i,k''}$. The cumulative distribution function of $\Omega_{i,k"}\triangleq\sin^2\left(\phi_{i,k''}\right)$ is given by [35]:

$$F_{\Omega_{i,k"}}\left(\varpi\right)=\begin{cases}1\ , & \text{if } 0\leq\varpi\leq 2^{-\frac{B}{N_t-1}},\ (A3)\\ 2^B\left(\varpi\right)^{N_t-1}, & \text{if } \varpi\geq 2^{-\frac{B}{N_t-1}}.\end{cases}$$

Hence, we have $\left\|\mathbf{f}_{i,k"}\right\|^2\sin^2\left(\phi_{i,k"}\right)\sim$ Gamma $\left(N_t-1,2^{-\frac{B}{N_t-1}}\right)$, which is gamma distributed with a shape parameter of N_t-1 and scale parameter of $2^{-\frac{B}{N_t-1}}$ [35, Lemma 1]. On the other hand, $\mathbf{e}_{i,k"}$ is a unit vector that has the same distribution as $\mathbf{f}_{i,k"}$. Moreover, the unit vector $\mathbf{w}_m$ is isotropic within the (N_t-1)-dimensional hyperplane and independent of $\mathbf{e}_{i,k"}$. Based on [28, Lemma 2], we have $\left|\mathbf{w}_m^H\mathbf{e}_{i,k"}\right|^2\sim$ Beta$\left(1,N_t{-}2\right)$. Therefore the product $\mathcal{Y}_{i,k"}=$ Beta$\left(1,N_t{-}2\right)\times$ Gamma $\left(N_t-1,2^{-\frac{B}{N_t-1}}\right)$ is exponentially distributed as [36, Lemma 1], $\mathcal{Y}_{i,k"}=\left\|\mathbf{f}_{i,k"}\right\|^2\sin^2\left(\phi_{i,k"}\right)\left|\mathbf{w}_m^H\mathbf{e}_{i,k"}\right|^2\sim\mathrm{Exp}\left(2^{\frac{B}{N_t-1}}\right)$. If we define the new variables $\bar{\mathcal{X}}_{m,k',n'}\sim\mathrm{Exp}\left(\lambda_{m,k',n'}=\frac{1}{2p_{m,k',n'}\mathrm{PL}\left(d_{m,k'}\right)}\right)$, $\bar{\mathcal{Y}}_{i,k''}\sim\mathrm{Exp}\left(\lambda_{i,k"}=\frac{2^{\frac{B}{N_t-1}}}{P_{i,k"}\mathrm{PL}\left(d_{i,k''}\right)}\right)$, then the $P_{m,k,n}^{CO}$ can be expressed as $(A4)$, where $\mathcal{L}_X\left(s\right)\triangleq\mathbb{E}\left\{e^{-sx}\right\}$ is the Laplace transform. Step (a) is reached by conditioning on the aggregate interference $\sum_{(k',n')\in\Phi_{m,k,n}}\bar{\mathcal{X}}_{m,k',n'}+\sum_{i=1,i\neq m}^{M}\sum_{k''=1}^{K_i}\bar{\mathcal{Y}}_{i,k''}$ and (b) by the independence of the interference terms.

APPENDIX B
DERIVATION OF (12)

Based on (9), $P_{j,k,n}^{SO}$ can be expressed as $(B1)$, where $\mathcal{W}_{j,k,n}\triangleq p_{m,k,n}\mathrm{PL}\left(d_{m,k,j}\right)\lambda_j^{max}\left\{\tilde{\mathbf{Q}}_{m,j}\right\}\left|g_{m,k,j}\right|^2$ and $\mathcal{U}_{j,k',n'}\triangleq p_{m,k',n'}\mathrm{PL}\left(d_{m,k',j}\right)\lambda_j^{max}\left\{\tilde{\mathbf{Q}}_{m,j}\right\}\left|g_{m,k',j}\right|^2$ are independent exponential r.v obeying the distribution of $\mathcal{W}_{j,k,n}\sim\mathrm{Exp}\left(\eta_{j,k,n}=\frac{1}{p_{m,k,n}\mathrm{PL}\left(d_{m,k,j}\right)\lambda_j^{max}\left\{\tilde{\mathbf{Q}}_{m,j}\right\}}\right)$ and $\mathcal{U}_{k',n}\sim\mathrm{Exp}\left(\zeta_{j,k',n'}=\frac{1}{p_{m,k',n'}\mathrm{PL}\left(d_{m,k',j}\right)\lambda_j^{max}\left\{\tilde{\mathbf{Q}}_{m,j}\right\}}\right)$. Then the $P_{j,k,n}^{SO}$ can be expressed as $(B2)$, where $\kappa_{j,k,n}\triangleq 2^{D_{j,k,n}}-1$.

REFERENCES

[1] M. Alzenad, A. El-Keyi, and H. Yanikomeroglu, "3-D placement of an unmanned aerial vehicle base station for maximum coverage of users with different QoS requirements," *IEEE Wireless Communications Letters*, vol. 7, no. 1, pp. 38–41, 2017.

[2] Y. Sun, D. Xu, D. W. K. Ng, L. Dai and R. Schober, "Optimal 3D-Trajectory Design and Resource Allocation for Solar-Powered UAV Communication Systems," *in IEEE Transactions on Communications*, vol. 67, no. 6, pp. 4281-4298, June 2019, doi: 10.1109/TCOMM.2019.2900630.

[3] W. Jaafar, N. Shimaa, M. Sami, C.S Paschalis, and H. Yanikomeroglu. "On the downlink performance of RSMA-based UAV communications." *IEEE Transactions on Vehicular Technology 69*, no. 12 (2020): 16258-16263.

[4] H. Zhang, J. Zhang and K. Long, "Energy Efficiency Optimization for NOMA UAV Network with Imperfect CSI," in *IEEE Journal on Selected Areas in Communications*, vol. 38, no. 12, pp. 2798-2809, Dec. 2020, doi: 10.1109/JSAC.2020.3005489.

[5] H. Bastami, M. Letafati, M. Moradikia, A. Abdelhadi, H. Behroozi and L. Hanzo, "On the Physical Layer Security of the Cooperative Rate-Splitting Aided Downlink in UAV Networks," *in IEEE Transactions on Information Forensics and Security*, doi: 10.1109/TIFS.2021.312298

[6] H. Bastami, M. Moradikia, M. Letafati, A. Abdelhadi, and H. Behroozi. "Outage-Constrained Robust and Secure Design for Downlink Rate-Splitting UAV Networks." *In 2021 IEEE International Conference on Communications Workshops (ICC Workshops)*, pp. 1-7, 2021.

[7] M. Kountouris, and J. G. Andrews. "Downlink SDMA with limited feedback in interference-limited wireless networks." *IEEE Transactions on Wireless Communications 11*, no. 8, 2012.

[8] Z. Li, M. Xia, M. Wen, and Y. Wu. "Massive access in secure NOMA under imperfect CSI: security guaranteed sum-rate maximization with first-order algorithm." *IEEE Journal on Selected Areas in Communications 39*, no. 4, 2020.

[9] Y. Mao, B. Clerckx, and V. O. Li, "Rate-splitting multiple access for downlink communication systems: bridging, generalizing, and outperforming SDMA and NOMA," *EURASIP journal on wireless communications and networking*, vol. 2018, no. 1, p. 133, 2018.

[10] H. Fu, S. Feng, W. Tang and D. W. K. Ng, "Robust Secure Beamforming Design for Two-User Downlink MISO Rate-Splitting Systems," *in IEEE Transactions on Wireless Communications*, vol. 19, no. 12, pp. 8351-8365, Dec. 2020.

[11] J. Zeng, T. Lv, W. Ni, R. P. Liu, N. C. Beaulieu and Y. J. Guo, "Ensuring Max–Min Fairness of UL SIMO-NOMA: A Rate Splitting Approach," *in IEEE Transactions on Vehicular Technology,* vol. 68, no. 11, pp. 11080-11093, Nov. 2019, doi: 10.1109/TVT.2019.2943511.

[12] O. Abbasi, and H. Yanikomeroglu, "Rate-Splitting and NOMA-Enabled Uplink User Cooperation." *In 2021 IEEE Wireless Communications and Networking Conference Workshops (WCNCW)* (pp. 1-6), 2021.

[13] Y. Mao, O. Dizdar, B. Clerckx, R. Schober, P. Popovski and H. V. Poor, "Rate-Splitting Multiple Access: Fundamentals, Survey, and Future Research Trends," in *IEEE Communications Surveys & Tutorials, 2022,* doi: 10.1109/COMST.2022.3191937.

[14] Z. Yang, M. Chen, W. Saad, W. Xu, and M. Shikh-Bahaei. "Sum-rate maximization of uplink rate splitting multiple access (RSMA) communication." *IEEE Transactions on Mobile Computing (2020).*

[15] Lu, Huabing *et al*. "Outage Performance of Uplink Rate Splitting Multiple Access with Randomly Deployed Users." *ArXiv abs/2204.14154 (2022).*

[16] M. Katwe, K. Singh, B. Clerckx and C. -P. Li, "Rate Splitting Multiple Access for Sum-Rate Maximization in IRS Aided Uplink Communications," *in IEEE Transactions on Wireless Communications*, 2022, doi: 10.1109/TWC.2022.3210338.

[17] S. Lin, T. Chang, Y. Hong and C. Chi, "On the Impact of Quantized Channel Direction Feedback in Multiple-Antenna Wiretap Channels," *2010 IEEE International Conference on Communications,* 2010, pp. 1-5, doi: 10.1109/ICC.2010.5502608.

[18] M. Moradikia, H. Bastami, A. Kuhestani, H. Behroozi, and L. Hanzo, "Cooperative secure transmission relying on optimal power allocation in the presence of untrusted relays, a passive eavesdropper and hardware impairments," *IEEE Access*, vol. 7, pp. 116 942–116 964, 2019.

[19] M. Moradikia, S. Mashdour, and A. Jamshidi. "Joint optimal power allocation, cooperative beamforming, and jammer selection design to secure untrusted relaying network." *Transactions on Emerging Telecommunications Technologies 29*, no. 3, 2018.

$$P_{m,k,n}^{CO} = 1 - \mathbb{P}\left\{ \beta_{m,n,k} \leq \frac{\bar{\mathcal{X}}_{m,k,n}}{\sum_{(k',n')\in\Phi_{m,k,n}} \bar{\mathcal{X}}_{m,k',n'} + \sum\limits_{i=1,i\neq m}^{M} \sum\limits_{k"=1}^{K_i} \bar{\mathcal{Y}}_{i,k"} + \sigma_m^2} \right\}$$
$$= 1 - \mathbb{P}\left\{ \bar{\mathcal{X}}_{m,k,n} \geq \beta_{m,n,k} \left(\sum_{(k',n')\in\Phi_{m,k,n}} \bar{\mathcal{X}}_{m,k',n'} + \sum_{i=1,i\neq m}^{M} \sum_{k''=1}^{K_i} \bar{\mathcal{Y}}_{i,k''} + \sigma_m^2 \right) \right\}$$
$$\overset{(a)}{=} 1 - \mathbb{E}\left\{ \exp\left(- \frac{\beta_{m,n,k} \left(\sum_{(k',n')\in\Phi_{m,k,n}} \bar{\mathcal{X}}_{m,k',n'} + \sum\limits_{i=1,i\neq m}^{M} \sum\limits_{k''=1}^{K_i} \bar{\mathcal{Y}}_{i,k''} + \sigma_m^2 \right)}{2} \right) \right\}$$
$$\overset{(b)}{=} 1 - \exp\left(-\frac{\beta_{m,n,k}\sigma_m^2}{2} \right) \prod_{(k',n')\in\Phi_{m,k,n}} \prod_{i=1,i\neq m}^{M} \prod_{k"=1}^{K_i} \left(\frac{\lambda_{m,k',n'}}{\lambda_{m,k',n'} + \frac{\beta_{m,n,k}}{2}} \right) \left(\frac{\lambda_{i,k''}}{\lambda_{i,k''} + \frac{\beta_{m,n,k}}{2}} \right), \quad (A4)$$

$$P_{j,k,n}^{SO} = \mathbb{P}\left\{ 2^{D_{j,k,n}} - 1 < \frac{p_{m,k,n}\mathrm{PL}\left(d_{m,k,j}\right)\left|g_{m,k,j}\right|^2}{\sum_{(k',n')\neq(k,n)} p_{m,k',n'}\mathrm{PL}\left(d_{m,k',j}\right)\left|g_{m,k',j}\right|^2 + \sigma_e^2} \right\} = \mathbb{P}\left\{ 2^{D_{j,k,n}} - 1 < \frac{\mathcal{W}_{j,k,n}}{\sum_{(k',n')\neq(k,n)} \mathcal{U}_{j,k',n'} + \sigma_e^2} \right\} \quad (B1)$$

$$P_{j,k,n}^{SO} = \mathbb{P}\left\{ \mathcal{W}_{j,k,n} > \kappa_{j,k,n} \left(\sum_{(k',n')\neq(k,n)} \mathcal{U}_{j,k',n'} + \sigma_e^2 \right) \right\} \overset{(a)}{=} \mathbb{P}\left\{ \exp\left(-\eta_{j,k,n}\kappa_{j,k,n} \left(\sum_{(k',n')\neq(k,n)} \mathcal{U}_{j,k',n'} + \sigma_e^2 \right) \right) \right\}, \quad (B2)$$
$$\overset{(b)}{=} \mathbb{E}\left\{ \exp\left(-\eta_{j,k,n}\kappa_{j,k,n}\sigma_e^2\right) \prod_{(k',n')\neq(k,n)} \mathcal{L}_{\mathcal{U}_{k',n}}\left(\eta_{j,k,n}\kappa_{j,k,n}\right) \right\} = \exp\left(-\eta_{j,k,n}\kappa_{j,k,n}\sigma_e^2\right) \prod_{(k',n')\neq(k,n)} \left(1 + \eta_{j,k,n}\kappa_{j,k,n}\zeta_{j,k',n'}^{-1}\right)^{-1},$$

[20] Y. Sun, D. W. K. Ng, J. Zhu and R. Schober, "Robust and Secure Resource Allocation for Full-Duplex MISO Multicarrier NOMA Systems," *in IEEE Transactions on Communications*, vol. 66, no. 9, pp. 4119-4137, Sept. 2018, doi: 10.1109/TCOMM.2018.2830325.

[21] Y. Li, M. Jiang, Q. Zhang, Q. Li and J. Qin, "Secure Beamforming in Downlink MISO Nonorthogonal Multiple Access Systems," *in IEEE Transactions on Vehicular Technology,* vol. 66, no. 8, pp. 7563-7567, Aug. 2017, doi: 10.1109/TVT.2017.2658563.

[22] R. M. Corless, G. H. Gonnet, D. E. G. Hare, D. J. Jeffrey, and D. E. Knuth, "On the Lambert W function," *Advances in Computational Mathematics*, vol. 5, no. 1, pp. 329–359, Dec. 1996.

[23] A. Omri and M. O. Hasna, "Physical Layer Security Analysis of UAV Based Communication Networks," *2018 IEEE 88th Vehicular Technology Conference (VTC-Fall)*, 2018, pp. 1-6, doi: 10.1109/VTC-Fall.2018.8690950.

[24] B. Mehlig and J. T. Chalker, "Statistical properties of eigenvectors in non-Hermitian Gaussian random matrix ensembles", *Journal of Mathematical Physics*, 2000, https://doi.org/10.1063%2F1.533302.

[25] B. Clerckx and C. Oestges, *MIMO Wireless Networks: Channels, Techniques and Standards for Multi-Antenna, Multi-User and Multi-Cell Systems*, 2nd ed. Academic Press, 2013.

[26] D. J. Love, R. W. Heath and T. Strohmer, "Grassmannian beamforming for multiple-input multiple-output wireless systems," *in IEEE Transactions on Information Theory*, vol. 49, no. 10, pp. 2735-2747, Oct. 2003, doi: 10.1109/TIT.2003.817466.

[27] K. K. Mukkavilli, A. Sabharwal, E. Erkip and B. Aazhang, "On beamforming with finite rate feedback in multiple-antenna systems," *in IEEE Transactions on Information Theory*, vol. 49, no. 10, pp. 2562-2579, Oct. 2003, doi: 10.1109/TIT.2003.817433.

[28] N. Jindal, "MIMO broadcast channels with finite-rate feedback," *IEEE Trans. Inf. Theory*, vol. 52, no. 11, pp. 5045–5060, Nov. 2006.

[29] A. Mishra, Y. Mao, O. Dizdar and B. Clerckx, "Rate-Splitting Multiple Access for 6G—Part I: Principles, Applications and Future Works," *in IEEE Communications Letters*, vol. 26, no. 10, pp. 2232-2236, Oct. 2022, doi: 10.1109/LCOMM.2022.3192012.

[30] B. Rimoldi and R. Urbanke, "A rate-splitting approach to the Gaussian multiple-access channel," *in IEEE Transactions on Information Theory,* vol. 42, no. 2, pp. 364-375, March 1996, doi: 10.1109/18.485709.

[31] J. C. Roh and B. D. Rao, "Transmit beamforming in multiple-antenna systems with finite rate feedback: a VQ-based approach," *in IEEE Transactions on Information Theory,* vol. 52, no. 3, pp. 1101-1112, March 2006, doi: 10.1109/TIT.2005.864426.

[32] W. Wang, K. C. Teh, and K. H. Li, "Secrecy throughput maximization for MISO multi-eavesdropper wiretap channels," *IEEE Trans. Inf. Forensics Security*, vol. 12, no. 3, pp. 505–515, Mar. 2017.

[33] F. Oggier and B. Hassibi, "The secrecy capacity of the MIMO wiretap channel," *IEEE Trans. Inf. Theory*, vol. 57, no. 8, pp. 4961–4972, Aug. 2011.

[34] A. Jeffrey and D. Zwillinger, *Table of Integrals, Series, and Products (6th ed.)*. San Diego, USA: Academic Press, 2000.

[35] T. Yoo, N. Jindal and A. Goldsmith, "Multi-Antenna Downlink Channels with Limited Feedback and User Selection," *in IEEE Journal on Selected Areas in Communications,* vol. 25, no. 7, pp. 1478-1491, September 2007, doi: 10.1109/JSAC.2007.070920.

[36] J. Zhang, R. W. Heath, M. Kountouris, and J. G. Andrews, "Mode switching for the multi-antenna broadcast channel based on delay and channel quantization," *EURASIP J. Adv. Sig. Proc.,* vol. 2009, no. 1, p. 802548, Jun. 2009.

[37] H. Bastami, H. Behroozi, M. Moradikia, A. Abdelhadi, D. W. K. Ngand, and L. Hanzo, " Large-Scale Rate-Splitting Multiple Access in Uplink UAV Networks: Effective Secrecy Throughput Maximization Under Limited Feedback Channel", 2022, *[online] Available: http://arxiv.org/submit/4512415/pdf*.

[38] H. Bastami, M. Moradikia, H. Behroozi, R. C. de Lamare, A. Abdelhadi, Z. Ding, "Secrecy rate maximization for hardware impaired untrusted relaying network with deep learning", *Physical Communication*, Volume 49, 2021, 101476, ISSN 1874-4907, https://doi.org/10.1016/j.phycom.2021.101476.

[39] S. Boyd and L. Vandenberghe, Convex Optimization. USA: *Cambridge University Press*, 2004.

[40] D. Bertsekas, Nonlinear Programming. Athena Scientific, 1999.